Acta Crystallographica Section F
Structural Biology and Crystallization Communications
ISSN 1744-3091

Crystallization of dihydrodipicolinate synthase from a clinical isolate of *Streptococcus pneumoniae*

Natalia E. Sibarani,[a,b] Michael A. Gorman,[c] Con Dogovski,[a,b] Michael W. Parker[a,b,c] and Matthew A. Perugini[a,b]*

[a]Department of Biochemistry and Molecular Biology, University of Melbourne, Parkville, Victoria 3010, Australia, [b]Bio21 Molecular Science and Biotechnology Institute, 30 Flemington Road, Parkville 3010, Australia, and [c]St Vincent's Institute of Medical Research, 9 Princes Street, Fitzroy, Victoria 3065, Australia

Correspondence e-mail: perugini@unimelb.edu.au

Received 19 August 2009
Accepted 11 November 2009

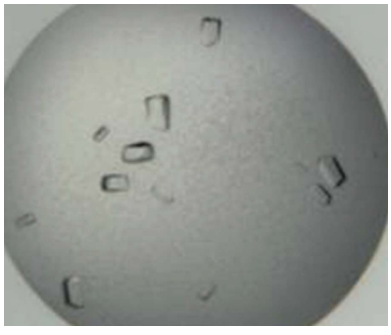

© 2010 International Union of Crystallography
All rights reserved

Dihydrodipicolinate synthase (DHDPS; EC 4.2.1.52) catalyzes the rate-limiting step in the (*S*)-lysine biosynthesis pathway of bacteria and plants. Here, the cloning of the DHDPS gene from a clinical isolate of *Streptococcus pneumoniae* (OXC141 strain) and the strategy used to express, purify and crystallize the recombinant enzyme are described. Diffracting crystals were grown in high-molecular-weight PEG precipitants using the hanging-drop vapour-diffusion method. The best crystal, from which data were collected, diffracted to beyond 2.0 Å resolution. Initially, the crystals were thought to belong to space group $P4_22_12$, with unit-cell parameters $a = 105.5$, $b = 105.5$, $c = 62.4$ Å. However, the R factors remained high following initial processing of the data. It was subsequently shown that the data set was twinned and it was thus reprocessed in space group $P2$, resulting in a significant reduction in the R factors. Determination of the structure will provide insight into the design of novel antimicrobial agents targeting this important enzyme from *S. pneumoniae*.

1. Introduction

The Gram-positive bacterium *Streptococcus pneumoniae* is the predominant causative agent of community-acquired pneumonia and otitis media worldwide (Cartwright, 2002). Those highly susceptible to infection by *S. pneumoniae* are the elderly, the immunocompromized and children. It has recently been estimated that over one million children die annually owing to *S. pneumoniae* infections (Rudan *et al.*, 2008; Scott *et al.*, 2008). In recent years, there has been a proliferation of multi-drug-resistant strains of this bacterium. This proliferation has coincided with the overuse and misuse of broad- and narrow-spectrum antibiotics (Andersson & Levin, 1999; Wegener, 2003). It is therefore urgent to discover novel antimicrobial agents that target antibiotic resistant bacteria, including strains of drug-resistant *S. pneumoniae* (DRSP). Of equal urgency is the need to characterize new antimicrobial targets. One such target is the (*S*)-lysine biosynthesis pathway in bacteria, which is absent in humans.

The (*S*)-lysine biosynthetic pathway provides bacteria with the essential building blocks for the formation of the bacterial cell wall and the synthesis of proteins (Hutton *et al.*, 2007). In Gram-positive bacteria such as *S. pneumoniae*, (*S*)-lysine is an integral component of the peptidoglycan cell wall (Scheffers & Pinho, 2005). The enzyme dihydrodipicolinate synthase (DHDPS) catalyzes the first committed step in the (*S*)-lysine biosynthesis pathway of bacteria, plants and some fungi (Hutton *et al.*, 2007). The catalytic mechanism of the enzyme has been extensively studied in numerous bacterial and plant species (Dobson, Gerrard *et al.*, 2004; Dobson, Griffin *et al.*, 2004, 2005; Dobson, Valegård *et al.*, 2004) and involves the aldol condensation of the substrates pyruvate and (*S*)-aspartate-β-semialdehyde to form the transient product (4*S*)-4-hydroxy-2,3,4,5-tetrahydro-(2*S*)-dipicolinic acid. The ability of DHDPS to be feedback-inhibited by its end product, (*S*)-lysine, is a phenomenon that is exhibited ubiquitously in plants (Matthews & Widholm, 1978; Wallsgrove & Mazelis, 1981; Kumpaisal *et al.*, 1987; Ghislain *et al.*, 1990; Frisch *et al.*, 1991; Dereppe *et al.*, 1992). To date, only the Gram-negative bacterium *Escherichia coli* demonstrates this form of regulation and thus the mechanism of (*S*)-lysine feedback regulation in bacteria remains

poorly understood (Yugari & Gilvarg, 1965; Stahly, 1969; Karsten, 1997; Dobson, Griffin *et al.*, 2004; Burgess *et al.*, 2008).

The crystal structures of bacterial DHDPS obtained to date have revealed the enzyme to be a homotetramer. The tetramer is described as a dimer of dimers (monomers *A* and *B* and monomers *C* and *D*; Fig. 1), with strong interactions between monomers *A* and *B* at the so-called tight-dimer interface and weaker interactions between the dimers at the weak-dimer interface (Mirwaldt *et al.*, 1995; Blickling *et al.*, 1997; Blagova *et al.*, 2005; Dobson, Griffin *et al.*, 2005; Perugini *et al.*, 2005; Pearce *et al.*, 2006; Kefala *et al.*, 2007; Burgess *et al.*, 2008; Fig. 1) However, an active dimeric form of DHDPS from *Staphylococcus aureus* has recently been described (Burgess *et al.*, 2008; Girish *et al.*, 2008). Despite these differences in quaternary architecture, the subunit structure of DHDPS is highly conserved across all species. The DHDPS monomer adopts a TIM-barrel or $(\beta/\alpha)_8$ folding topology, with the active site located within the centre of the barrel (Mirwaldt *et al.*, 1995; Dobson, Griffin *et al.*, 2005; Fig. 1). In the case of tetrameric DHDPS, four active sites are present in the enzyme and adjacent to these active sites, located in a cleft formed at the tight-dimer interface, is the location of the allosteric site to which (*S*)-lysine binds (Fig. 1).

The active-site region is highly conserved throughout DHDPS enzymes; however, little conservation is observed amongst bacterial species towards the periphery of the tetramer and at the weak-dimer interface (Fig. 1). Mutants constructed of *E. coli* DHDPS that disrupt the tetrameric structure and stabilize the tight-dimer form confer markedly reduced catalytic activity (Griffin *et al.*, 2008). Loss of activity has also recently been described for dimeric mutants of DHDPS from *Bacillus anthracis* (Voss *et al.*, 2009). Thus, the weak-dimer interface is of great interest as this region proves an attractive target for potential pathogen-specific therapeutics given the minimal sequence conservation at this interface between species. Another region of DHDPS that has yet to be exploited for the design of therapeutics is the (*S*)-lysine-binding or allosteric site (Fig. 1). Although DHDPS from Gram-positive species characterized to date lack (*S*)-lysine feedback inhibition (Hutton *et al.*, 2007; Burgess *et al.*, 2008; Voss *et al.*, 2009), sequence analysis indicates that the allosteric site residues of DHDPS from *E. coli* are conserved in *S. pneumoniae*. Accordingly, we aim to determine the crystal structure of DHDPS from *S. pneumoniae* as the first step in a structure-based drug-design program. Here, we describe the cloning, expression, purification, crystallization and preliminary X-ray crystallographic data of DHDPS from the OXC141 strain of *S. pneumoniae*. The crystal structure of the recombinant enzyme will provide insight into the activity and regulation of the enzyme and the design of novel antimicrobial agents targeting the enzyme from an important pathogen.

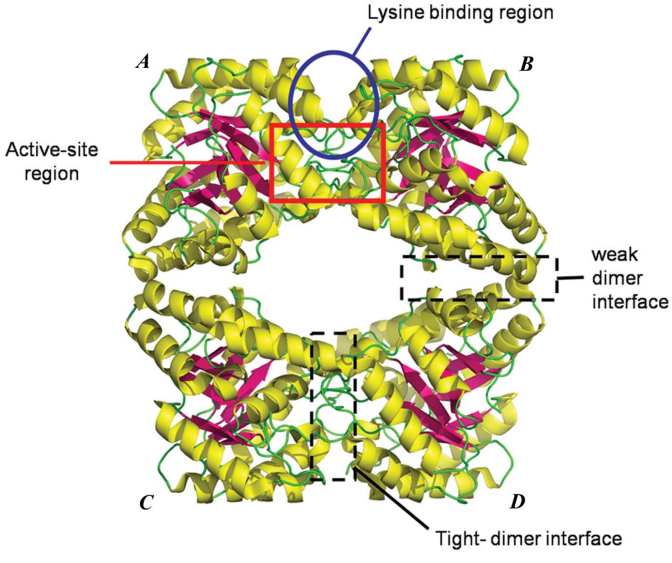

Figure 1
Crystal structure of dihydrodipicolinate synthase from *E. coli* (PDB code 1dhp; Mirwaldt *et al.*, 1995).

2. Materials and methods

2.1. Gene cloning

The *Sp*-DHDPS gene (*Sp-dapA*) was amplified *via* PCR from the genomic DNA of a clinical isolate of *S. pneumoniae* (OXC141) using the forward primer 5′-CTCAAAGGTGCTGCTTGGAAC-3′ and the reverse primer 5′-TCAACTACCCTATTCAAACGCC-3′ located approximately 50 bp upstream and downstream, respectively, of the *dapA* gene. The amplified product was cloned into a pCR-Blunt II-TOPO (Invitrogen), producing the construct pNS01. The presence of the *Sp-dapA* gene was confirmed by agarose-gel electrophoresis and dideoxynucleotide sequencing. *Sp-dapA* was then subcloned into the *E. coli* expression vector Champion pET101/D-TOPO (Invitrogen) using the forward primer 5′-CTTCCTCTATATGTATCCCACAGA-ATAGTTC-3′ and the reverse primer 5′-GAAGGAGATATACAT-AGGGTGTCTTATCAAG-3′ to produce pNS02.

2.2. Protein expression and purification

The native recombinant protein was overexpressed in *E. coli* BL21 (DE3). Cells were grown at 310 K in Luria Broth containing ampicillin (75 µg ml^{-1}) to an OD_{600} of 0.6. The cells were subsequently treated with 1.0 m*M* IPTG for 3 h to induce recombinant protein expression and then harvested at 277 K by centrifugation at 10 000*g* for 17 min. The cell pellets were stored at 253 K prior to purification.

Cell pellets were thawed at 277 K and resuspended in 20 m*M* Tris pH 8.0 (buffer *A*). Once thawed, pellets were lysed *via* a 6 min sonication cycle (3 s bursts, 10 s rests) using an MSE Soniprep 150 sonicator at an amplitude of 14 µm. The lysate was clarified by centrifugation at 7000*g* for 17 min at 277 K followed by passage of the supernatant through a 0.45 µm filter (Millipore). The recombinant enzyme was purified employing a two-step procedure consisting of anion-exchange liquid chromatography followed by size-exclusion liquid chromatography. A Q-Sepharose anion-exchange column (50 ml bed volume, 10 cm) was equilibrated at 277 K with buffer *A* prior to loading of the cell lysate. Once loaded onto the column, the column was washed with buffer *A* until a stable baseline was obtained. Protein elution was achieved by running a gradient of 20 m*M* Tris, 1.0 *M* NaCl pH 8.0 over five column volumes, collecting 10 ml fractions. The presence of *Sp*-DHDPS was detected using the colorimetric *o*-aminobenzaldehyde DHDPS enzyme-activity assay (Dobson, Devenish *et al.*, 2005) and SDS–PAGE. Fractions containing *Sp*-DHDPS were pooled and concentrated *via* centrifugation at 3000*g* and 277 K using a Centricon (30 kDa molecular-weight cutoff) until the protein concentration of *Sp*-DHDPS was 30 mg ml^{-1}. The concentrated enzyme was then loaded onto a 10/300 Sephacryl S-200 size-exclusion column (GE Healthcare) and 0.5 ml fractions were collected. Once again, the presence of *Sp*-DHDPS was detected using the *o*-aminobenzaldehyde assay (Dobson, Devenish *et al.*, 2005) and SDS–PAGE.

2.3. Protein crystallization

Purified *Sp*-DHDPS at a concentration of 10.0 mg ml^{-1} in 20 m*M* Tris–HCl, 150 m*M* NaCl pH 8.0 underwent initial crystallization screens at the CSIRO node of the Bio21 Collaborative Crystallization Centre (C3; http://www.csiro.au/c3/) using the PACT Suite and the JCSG+ Suite crystal screens (Qiagen) at 281 and 293 K (Newman *et al.*, 2005). These initial screens were set up in 96-well plates using the sitting-drop vapour-diffusion method. Each drop contained 100 nl protein solution and 100 nl reservoir solution. Initial screens yielded several microcrystals at both temperatures after 1 d, predominately in reservoir conditions containing the high-molecular-weight PEG precipitants PEG 6000 and PEG 3350. The crystals were predominately cubic in shape and the largest crystal was approximately 0.05 mm in size. From these initial screens, 12 conditions were selected and used on a larger scale in 24-well Linbro plates (Hampton Research) with the hanging-drop vapour-diffusion method at 293 K.

2.4. Data collection and processing

Diffraction data were collected on the Australian Synchrotron beamline MX1 using the program *Blu-Ice* (McPhillips *et al.*, 2002). Intensity data were collected at 100 K on an ADSC Q210r image-plate detector positioned at a distance of 199.97 mm. A 360° data set was collected with an oscillation angle of 0.5° and an exposure time of 5 s per diffraction image. Data were integrated using *HKL*-2000 (Otwinowski & Minor, 1997) and scaled using the program *SCALA* (Evans, 2006).

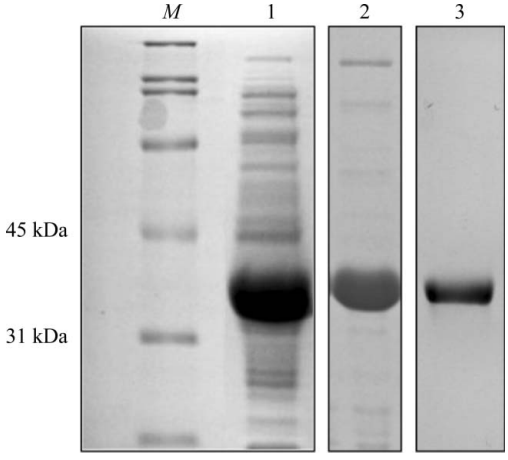

Figure 2
A 12% SDS–PAGE gel run to assess the effectiveness of the purification procedure. Lane *M*, marker proteins; lane 1, cell lysate (post-induction); lane 2, Q-Sepharose pooled *Sp*-DHDPS fractions; lane 3, Sephacryl S-200 pooled *Sp*-DHDPS fractions.

Table 1
Purification and activity of recombinant *Sp*-DHDPS.

Fraction	Volume (ml)	[Protein] (mg ml^{-1})	Protein (mg)	Activity (U ml^{-1})	Specific activity (U mg^{-1})	Purification factor (fold)
Crude	5.00	22.3	112	18.0	0.81	1.0
Q-Sepharose	20.0	4.50	90.6	4.03	0.89	1.1
Sephacryl S-200	4.00	2.80	11.2	4.52	1.61	2.0

3. Results and discussion

3.1. Purification and characterization of *Sp*-DHDPS

Recombinant *Sp*-DHDPS was expressed and purified as described in §2.2. The purity (Fig. 2) and enzymatic activity (Table 1) of the recombinant product was assessed in the crude cell lysate and following both liquid-chromatography steps of the purification procedure. The purified recombinant *Sp*-DHDPS product was estimated to be >95% pure (Fig. 2, lane 3) with a specific activity of 1.61 U mg^{-1} and an overall twofold purification (Table 1). Electrospray ionization time-of-flight (ESI-TOF) mass-spectrometric analysis of the purified enzyme (Fig. 3) shows that the mass of the recombinant product is 33 780.38 Da, which is in excellent agreement with the theoretical mass of the monomer (33 780.7 Da). Additional adducts are also observed in the deconvoluted mass spectrum of *Sp*-DHDPS that correspond to buffer salt adducts, namely sodium (Fig. 3). The purity and yield of the recombinant enzyme were therefore deemed to be suitable for crystallization trials.

3.2. Crystallization of *Sp*-DHDPS

Sp-DHDPS was initially screened for crystallization as described in §2.3. Larger crystals were then grown in-house under the optimized conditions selected from successful high-throughput screening trials (Fig. 4). The crystals shown in Fig. 4 were obtained by mixing 1 µl protein solution (10 mg ml^{-1}) with 1 µl reservoir solution [0.2 *M* ammonium chloride, 20%(*w*/*v*) PEG 6000, 0.1 *M* MES pH 6.0] at 293 K. Crystals were soaked briefly in cryoprotectant composed of 0.2 *M* ammonium chloride, 20%(*w*/*v*) PEG 6000, 0.1 *M* MES pH 6.0 and 20%(*w*/*v*) glycerol and were then flash-frozen using liquid nitrogen.

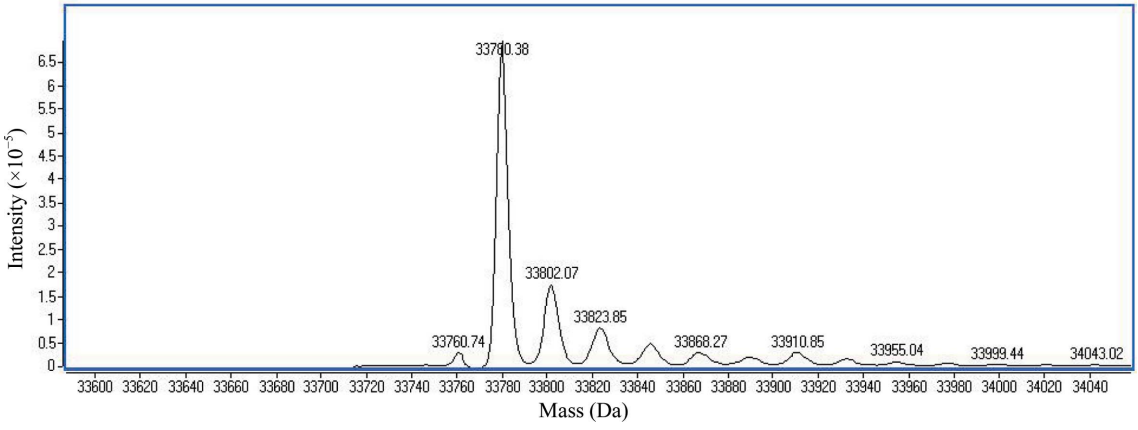

Figure 3
Deconvoluted ESI-TOF mass spectrum of purified recombinant *Sp*-DHDPS.

3.3. X-ray diffraction data

Fig. 5 shows an X-ray diffraction image to a resolution of 2.1 Å generated from an *Sp*-DHDPS crystal using the MX1 beamline at the Australian Synchrotron. Inspection of the systematic absences indicated that the crystal belonged to space group $P4_22_12$, with unit-cell parameters $a = b = 105.5$, $c = 62.4$ Å. The structure was successfully solved by molecular replacement using the program *Phaser* (McCoy *et al.*, 2005) with a model of DHDPS from *B. anthracis* (PDB code 1xl9; Blagova *et al.*, 2005). Despite multiple rounds of model building using *Coot* (Emsley & Cowtan, 2004) and refinement using *REFMAC*5 (Murshudov *et al.*, 1997), the *R* factors remained relatively high (*R* factor = 36.9%, R_{free} = 43.3%) and there were numerous spurious peaks in the $F_o - F_c$ difference maps. Analysis of the diffraction data using *phenix.xtrige* (Adams *et al.*, 2002) together with the output from *SCALA* indicated abnormal intensity statistics, suggesting overmerging of pseudosymmetric or twinned data. As there are no twin laws possible for this crystal system, the diffraction data were re-integrated and scaled in lower crystal systems and the statistics were inspected. The final space group was found to be *P*2 (Table 2), with twin law $-h$, $-k$, l. Initial refinement using *phenix.refine* produced clearer electron-density maps and lowered the *R* factors significantly (*R* factor = 28.5%, R_{free} = 33.2%). Further refinement is being carried out.

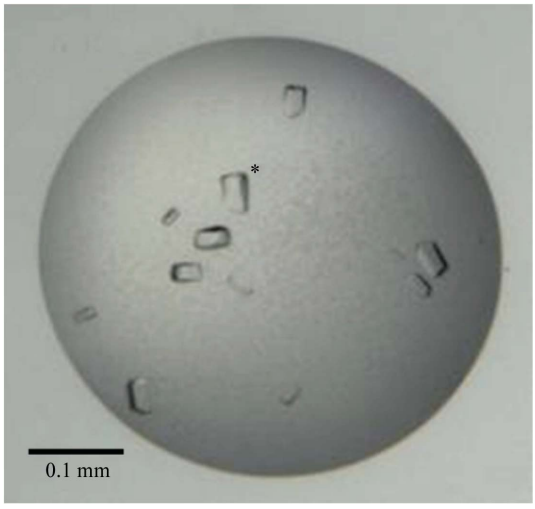

Figure 4
Crystal of recombinant *Sp*-DHDPS. The approximate length of the crystal is 0.04 mm. The crystal from which data were collected is marked with an asterisk.

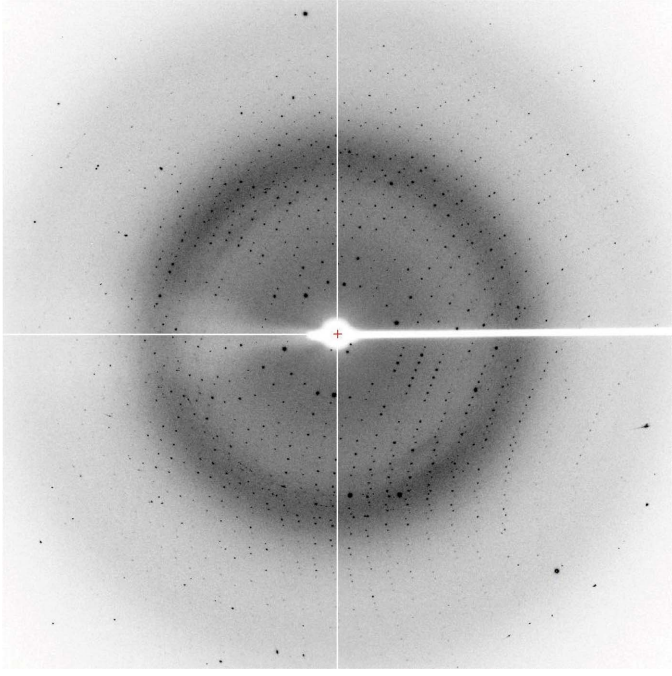

Figure 5
X-ray diffraction image from the crystal of *Sp*-DHDPS marked with an asterisk in Fig. 4.

Table 2
Data-collection and processing statistics.

Values in parentheses are for the highest resolution bin (2.06–1.99 Å).

Wavelength (Å)	0.9536
No. of images	720
Space group	*P*2
Unit-cell parameters (Å, °)	$a = 105.5$, $b = 62.4$, $c = 105.5$, $\beta = 90.02$
Resolution (Å)	50–1.99
Multiplicity	7.5 (7.1)
Completeness (%)	99.8 (89.5)
R_{merge}†	0.057 (0.408)
Mean $I/\sigma(I)$	34.12 (5.39)

† $R_{merge} = \sum_{hkl}\sum_i |I_i(hkl) - \langle I(hkl)\rangle| / \sum_{hkl}\sum_i I_i(hkl)$, where $I_i(hkl)$ is the *i*th observation of reflection *hkl* and $\langle I(hkl)\rangle$ is the weighted average intensity for all observations *i* of reflection *hkl*.

We would firstly like to acknowledge Associate Professor Geoff Hogg from the Microbiological Diagnostic Unit, University of Melbourne, Public Health Laboratory Network, Department of Health and Ageing, Australia for providing genomic DNA from *S. pneumoniae* (OXC141 strain). We would also like to acknowledge the support and assistance of the friendly staff at the Bio21 Collaborative Crystallographic Centre at CSIRO Molecular and Health Technologies, Parkville, Melbourne as well as all members of the Perugini laboratory for helpful discussions during the preparation of this manuscript. This research was undertaken using the MX1 beamline at the Australian Synchrotron, Victoria, Australia. The views expressed herein are those of the authors and are not necessarily those of the owner or operator of the Australian Synchrotron. Finally, we acknowledge the Defense Threat Reduction Agency (DTRA; Project ID AB07CBT004) for program funding and the Australian Research Council for providing a Future Fellowship to MAP and a Federation Fellowship to MWP.

References

Adams, P. D., Grosse-Kunstleve, R. W., Hung, L.-W., Ioerger, T. R., McCoy, A. J., Moriarty, N. W., Read, R. J., Sacchettini, J. C., Sauter, N. K. & Terwilliger, T. C. (2002). *Acta Cryst.* D**58**, 1948–1954.
Andersson, D. I. & Levin, B. R. (1999). *Curr. Opin. Microbiol.* **2**, 489–493.
Blagova, E., Levdikov, V., Milioti, N., Fogg, M. J., Kalliomaa, A. K., Brannigan, J. A., Wilson, K. S. & Wilkinson, A. J. (2005). *Proteins*, **62**, 297–301.
Blickling, S., Beisel, H. G., Bozic, D., Knablein, K., Laber, B. & Huber, R. (1997). *J. Mol. Biol.* **274**, 608–621.
Burgess, B. R., Dobson, R. C. J., Bailey, M. F., Atkinson, S. C., Griffin, M. D. W., Jameson, G. B., Parker, M. W., Gerrard, J. A. & Perugini, M. A. (2008). *J. Biol. Chem.* **283**, 27598–27603.
Cartwright, K. (2002). *Eur. J. Pediatr.* **161**, 188–195.
Dereppe, C., Bold, G., Ghisalba, O., Ebert, E. & Schar, H. P. (1992). *Plant. Physiol.* **98**, 813–821.
Dobson, R. C. J., Devenish, S. R. A., Turner, L. A., Clifford, V. R., Pearce, F. G., Jameson, G. B. & Gerrard, J. A. (2005). *Biochemistry*, **44**, 13007–13013.
Dobson, R. C. J., Gerrard, J. A. & Pearce, F. G. (2004). *Biochem. J.* **377**, 757–762.

Dobson, R. C. J., Griffin, M. D. W., Jameson, G. B. & Gerrard, J. A. (2005). *Acta Cryst.* D**61**, 1116–1124.
Dobson, R. C. J., Griffin, M. D. W., Roberts, S. J. & Gerrard, J. A. (2004). *Biochimie*, **86**, 311–315.
Dobson, R. C. J., Valegård, K. & Gerrard, J. A. (2004). *J. Mol. Biol.* **338**, 329–339.
Emsley, P. & Cowtan, K. (2004). *Acta Cryst.* D**60**, 2126–2132.
Evans, P. (2006). *Acta Cryst.* D**62**, 72–82.
Frisch, D. A., Gengenbach, B. G., Tommey, A. M., Sellner, J. M., Somers, D. A. & Myers, D. E. (1991). *Plant. Physiol.* **96**, 444–452.
Ghislain, M., Frankard, V. & Jacobs, M. (1990). *Planta*, **180**, 480–486.
Girish, T. S., Sharma, E. & Gopal, B. (2008). *FEBS Lett.* **582**, 2923–2930.
Griffin, M. D. W., Dobson, R. C. J., Pearce, F. G., Antonio, L., Whitten, A. E., Liew, C. K., Mackay, J. P., Trewhella, J., Jameson, G. B. & Perugini, M. A. (2008). *J. Mol. Biol.* **380**, 691–703.
Hutton, C. A., Perugini, M. A. & Gerrard, J. A. (2007). *Mol. Biosyst.* **3**, 458–465.
Karsten, W. E. (1997). *Biochemistry*, **36**, 1730–1739.
Kefala, G., Evans, G., Griffin, M. D. W., Devenish, S. R. A., Perugini, M. A., Gerrard, J. A., Weiss, M. S. & Dobson, R. C. J. (2007). *Biochem. J.* **411**, 351–360.
Kumpaisal, R., Hashimoto, T. & Yamada, Y. (1987). *Plant. Physiol.* **85**, 145–151.
Matthews, B. F. & Widholm, J. M. (1978). *Planta*, **141**, 315–321.
McCoy, A. J., Grosse-Kunstleve, R. W., Storoni, L. C. & Read, R. J. (2005). *Acta Cryst.* D**61**, 458–464.
McPhillips, T. M., McPhillips, S. E., Chiu, H.-J., Cohen, A. E., Deacon, A. M., Ellis, P. J., Garman, E., Gonzalez, A., Sauter, N. K., Phizackerley, R. P., Soltis, S. M. & Kuhn, P. (2002). *J. Synchrotron Rad.* **9**, 401–406.
Mirwaldt, C., Korndorfer, I. & Huber, R. (1995). *J. Mol. Biol.* **246**, 227–239.
Murshudov, G. N., Vagin, A. A. & Dodson, E. J. (1997). *Acta Cryst.* D**53**, 240–255.
Newman, J., Egan, D., Walter, T. S., Meged, R., Berry, I., Ben Jelloul, M., Sussman, J. L., Stuart, D. I. & Perrakis, A. (2005). *Acta Cryst.* D**61**, 1426–1431.
Otwinowski, Z. & Minor, W. (1997). *Methods Enzymol.* **276**, 307–326.
Pearce, F. G., Perugini, M. A., McKerchar, H. J. & Gerrard, J. A. (2006). *Biochem. J.* **400**, 359–366.
Perugini, M. A., Griffin, M. D. W., Smith, B. J., Webb, L. E., Davis, A. J., Handman, E. & Gerrard, J. A. (2005). *Eur. Biophys. J.* **34**, 469–476.
Rudan, I., Boschi-Pinto, C., Biloglav, Z., Mulholland, K. & Campbell, H. (2008). *Bull. World Health Organ.* **86**, 408–416.
Scheffers, D. J. & Pinho, M. G. (2005). *Microbiol. Mol. Biol. Rev.* **69**, 585–607.
Scott, J. A., Brooks, W. A., Peiris, J. S., Holtzman, D. & Mulholland, E. K. (2008). *J. Clin. Invest.* **118**, 1291–1300.
Stahly, D. P. (1969). *Biochim. Biophys. Acta*, **191**, 439–451.
Voss, J. E., Scally, S. W., Taylor, N. L., Griffin, M. D. W., Hutton, C. A., Parker, M. W., Alderton, M. R., Gerrard, J. A., Dobson, R. C. J., Dogovski, C. & Perugini, M. A. (2009). In the press.
Wallsgrove, R. M. & Mazelis, M. (1981). *Phytochemistry*, **20**, 2651–2655.
Wegener, H. C. (2003). *Curr. Opin. Microbiol.* **6**, 439–445.
Yugari, Y. & Gilvarg, C. (1965). *J. Biol. Chem.* **240**, 4710–4716.